Large-Scale Transient Simulations of Breast Cancer Tumour's Reflections using a 31-Element Conformal Array

Christophe Fumeaux [1], Maciej Klemm [2], Dirk Baumann [3]

[1]*School of Electrical and Electronic Engineering, University of Adelaide, Australia*
[1]cfumeaux@eleceng.adelaide.edu.au
[2]*Department of Electrical and Electronic Engineering, University of Bristol, United Kingdom*
m.klemm@bristol.ac.uk
[3]*Laboratory for Electromagnetic Fields and Microwave Electronics, ETH Zurich, Switzerland*
dbaumann@ifh.ee.ethz.ch

***Abstract* — This paper demonstrates large-scale electromagnetic simulations of a real microwave imaging system for breast cancer detection. In particular we present calculated transient scattering responses from a tumour in a breast phantom modelled with dispersive materials. The responses are obtained from the full-scale numerical model of the 31-element antennas array. Two different numerical methods are considered in this work, i.e. the Finite Integration Technique (FIT) method implemented in a commercial solver and an in-house developed Finite-Volume Time-Domain (FVTD) code.**

***Index Terms* — Microwave imaging, ultra-wideband antennas, antenna array, computational electromagnetics .**

I. Introduction

In this paper we focus on the large-scale numerical modelling of the microwave-radar imaging system developed at the University of Bristol and recently reported in [1, 2]. In radar-based imaging, the goal is to create a map of microwave scattering arising from the contrast in dielectric properties within the breast. The accurate numerical modelling of the full system, including a breast phantom, is a crucial step to support further development of the microwave imaging. Our considerations are relevant not only to the radar imaging technique, but also to a tomographic approach.

From the electromagnetic (EM) point of view the most important part of the imaging system is the antenna array. Until recently numerical models of arrays were limited to simple Hertzian sources or dipole antennas [3, 4]. However, by adding more elements into the array, and by choosing more complex antennas with tailored ultra-wide band (UWB) performance, one can achieve a significant improvement in imaging performance [5]. We believe that further development of microwave imaging systems will require extensive numerical EM modelling of the complete imaging system with accurate models of complex antennas, as well as advanced breast phantoms composed of realistically modelled biological tissue. This ability to increase the modelling accuracy of imaging systems will be especially crucial in forward models for 3D tomographic reconstructions.

To simulate radar imaging systems relying on pulsed UWB operation one naturally thinks of time-domain methods. In the present investigation, two distinct time-domain full-wave numerical methods are applied for evaluation and to cross-validate the results.

In a recent study [6] we considered simulations of the single antenna as well as transmission between two antennas across a dispersive breast phantom model. In the present contribution we extend the considerations to present large-scale EM simulations of the complete 31-antenna array with a homogeneous and dispersive breast phantom model. For a few chosen antennas from the array we will present: a) the direct coupling between antennas in the presence of the breast phantom, b) the extracted tumour's response and c) a comparison between simulations and phantom measurements presenting reflections from a tumour recorded by different antennas.

II. Simulation Methods

The full simulation of the imaging system, including the 31-antenna conformal array and phantom, is very involved by today's standards in full-wave computational electromagnetics. Experimental validation of the results is also extremely challenging, as a fully deterministic approach for this inverse scattering problem is not possible. Therefore, two different simulation methods are applied in parallel for cross-validation and verification. Time-domain numerical methods with domain discretization are preferred tools in this case, as this class of methods appears best suited for modelling UWB operation in the presence of inhomogeneous dispersive materials.

The first method used in this study is the Finite Integration Technique (FIT) introduced in [7]. This method is one of the most commonly applied time-domain methods for electromagnetic simulations. Implementations are usually based on a rectangular cell discretization, which makes the method very similar to the Finite-Difference Time-Domain (FDTD) [8]. The regular Cartesian discretization is very advantageous to achieve second-order accuracy in space and time at a minimal computational cost per cell, and eases parallelization. The commercial code used in the present study is CST Microwave Studio®, which incorporates special boundary treatment at curved and slanted material interfaces.

The second method applied to the conformal array is the Finite-Volume Time-Domain (FVTD) method [9]. FVTD can

be applied in unstructured polyhedral meshes, e.g. tetrahedral meshes. This is a feature shared by other conformal time-domain methods, such as the Discontinuous-Galerkin Time-Domain (DG-TD) method [10]. The use of potentially strongly inhomogeneous meshes is particularly advantageous for modelling problems with small details embedded in a larger structure [11-13]. The present implementation is an in-house developed FVTD tool that incorporates local time steps to match spatial discretization inhomogeneities [14]. For the problem at hand, the code makes use of specific treatments for dispersive materials [15], and truncates the computational domain with conformal perfectly-matched absorbers [16] around the antennas and at the base of the breast phantom.

III. 31-Element UWB Antenna Array

A. Geometry

The antenna array of the radar imaging system is comprised of 31 wide-slot UWB antennas. The conformal array is formed around a hemisphere with 85 mm radius. To provide the best radiation coverage of a breast, all antennas are positioned to point towards the centre of curvature. A plastic shell with openings for the antennas has been manufactured to assure the best possible accuracy when positioning the antennas. The photo of the array from a prototype imaging system and the equivalent numerical model are shown in Fig. 1. In normal operation conditions all antennas are immersed in a matching liquid with dielectric constant of around 9. It should be noted that the plastic support cup is not included in the numerical model.

B. Numerical Models

Fig. 2 presents a schematic of the numerical model for the complete 31-element antennas array with dispersive breast phantom. The model includes a tumour with a 6 mm diameter. As in the real imaging system, the antennas in the numerical model are immersed in the matching liquid, assumed to be lossless with $\varepsilon_r = 9$. The breast model is made of homogeneous fatty tissue covered by a 2 mm thick skin layer. Both biological tissues are dispersive with Debye model parameters as follows: skin ($\varepsilon_s = 37$, $\varepsilon_\infty = 4$, $\tau = 7.2$ ps), fatty breast tissue ($\varepsilon_s = 10$, $\varepsilon_\infty = 7$, $\tau = 7$ ps). The tumour phantom is modelled as non-dispersive lossy dielectric sphere with $\varepsilon_r = 50$ and conductivity of 7 S/m.

The computational cost associated with the full array simulation has been discussed and quantified in [6], and is summarized in Table I. The main challenge for the FIT is the resolution of the fine features of the antennas, especially when tilted in the conformal array configuration. The main challenge for FVTD is the large homogeneous domains meshed in tetrahedrons. The inhomogeneity of the FVTD mesh is exploited to resolve fine features and denser media, as illustrated in Fig. 3.

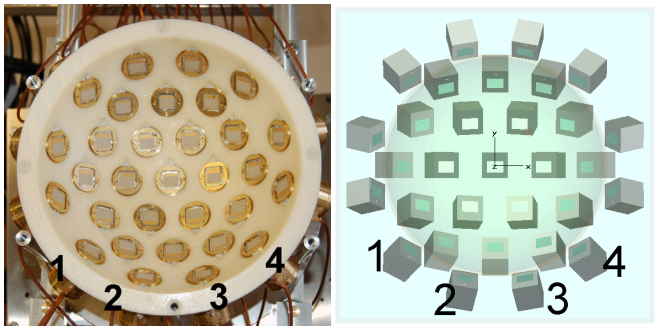

Fig. 1. Left: Photograph of the imaging system showing the 31 antennas conformally positioned in a plastic half-sphere. Right: Geometry of the equivalent numerical model, with indication of 4 selected antennas.

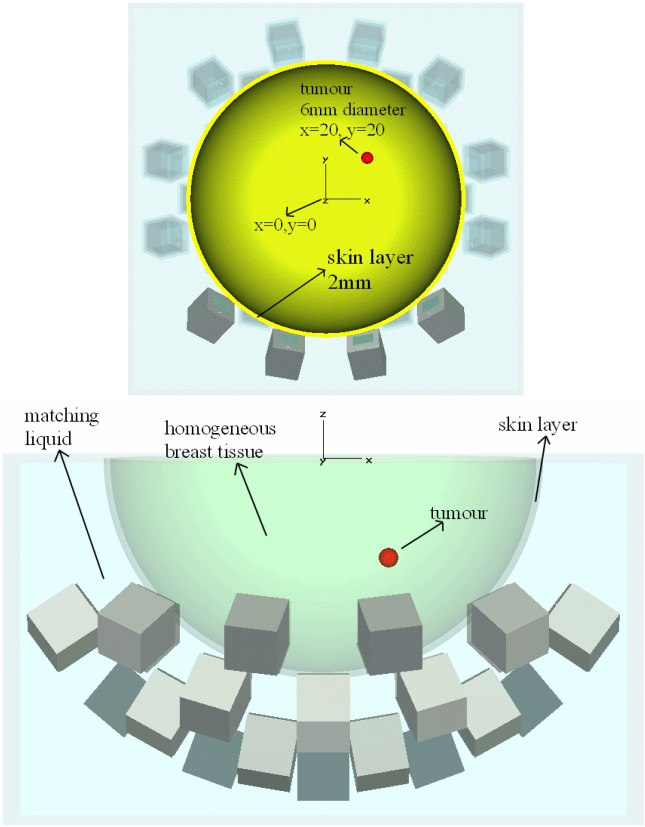

Fig. 2. Numerical FIT model of the complete 31-element antennas array with dispersive breast phantom and 6 mm diameter tumour: top view (upper image), side view (lower image).

TABLE I

Computational Costs for the Arrray with Phantom shown in Fig. 2

Numerical Model	**FVTD**	**FIT**
# mesh cells	22 M	>800 M (450 M [2])
Memory	25 GB	>48 GB (40 GB [2])
CPU time (for 5 ns) [1]	404 h	N/A (504 h [2])

[1] FVTD computations were performed on a single core of a Intel Xeon E5620 @ 2.40 GHz. FIT computations were performed on two quad core Intel Xeon E5405 @ 2.0GHz (8 cores used in total).

[2] FIT computations achieved by dividing the problem into three parts. Numbers shown are for the first partitioned sub-model (Tx = 1, Rx = 2:11).

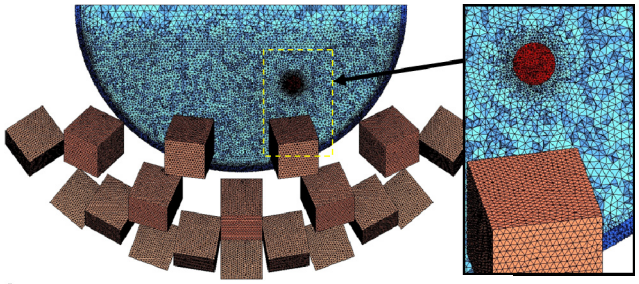

Fig. 3. Cut through the FVTD tetrahedral mesh for the breast phantom. The surface mesh of the antenna array is included. The inset shows the inhomogeneous mesh with refinement close to the denser tumour (red) and skin layer (darker blue)

IV. Results

In the real-life scenario the full scan using the prototype imaging system (Fig. 1) involves performing 465 S_{21} measurements using a network vector analyser, where each antenna transmits to all other antennas in a turn, and reciprocity is exploited to avoid redundant measurements. The equivalent "numerical scan" would involve 31 large-scale EM simulations. In this study we present results for the case where antenna 1 (as defined in Fig. 1) acts as a transmitter (Tx). All remaining antennas act as receivers (Rx). For the sake of brevity, only results for Rx = 2, 3 and 4 are presented here, but consistent results are obtained for other Tx-Rx pairs.

A. Direct coupling between antennas

The results presented in Fig. 4 show pulses transmitted between three different antenna pairs: a) Tx = 1, Rx = 2, b) Tx = 1, Rx = 3, c) Tx = 1, Rx = 4. The numerical model included the breast phantom as in Fig. 2, however without the tumour. Looking at time-of-arrival and shapes of transmitted pulses, a very good agreement was achieved with correlations of 94% for antenna pair a), 98% for b) and 80% for c).

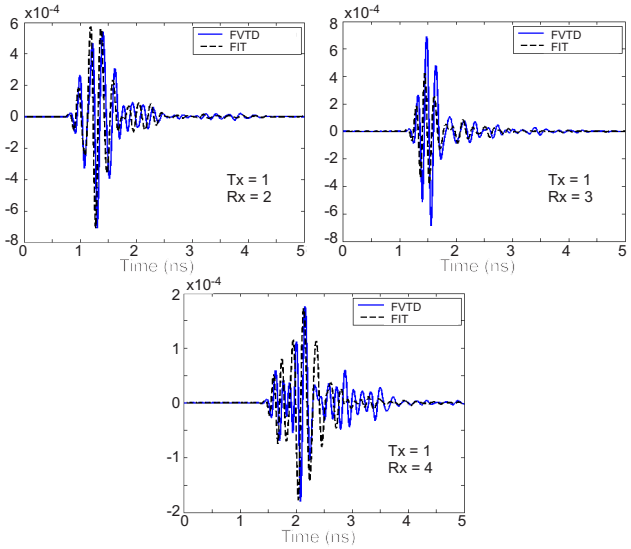

Fig. 4. Transmitted pulses (arbitrary units) between three UWB antenna pairs when irradiating the dispersive breast phantom.

B. Tumour's response

Figure 5 shows the extracted tumour responses, calculated by comparing transmitted pulses with and without tumour. Specifically, the scattering by the tumour was calculated as the difference in response between numerical models with and without the tumour. All results are on the same absolute scales and can be compared quantitatively.

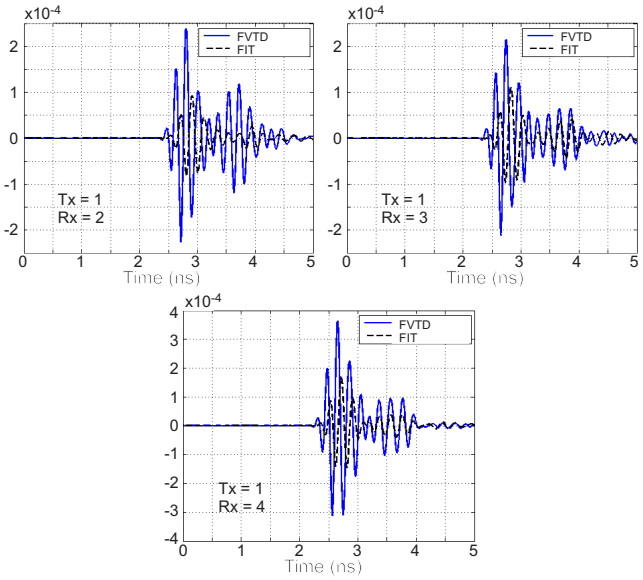

Fig. 5. Tumour's response extracted for different antennas pairs (FVTD: solid blue line, FIT: dashed black line).

For the results presented in Fig. 5, we observe that pulses calculated by FVTD have higher amplitudes by about 80-100%. The main reason for this is the better antenna matching in FVTD, allowed by accurate meshing of the fine details of the feeding structure. In FVTD, all antenna elements have exactly the same tetrahedral mesh (with appropriate orientation), which provides a consistent antenna performance (e.g. input matching) across the whole array. In FIT in the present model, each antenna has sightly different mesh and thus varying performance [6]. We also believe that a small difference in pulses' amplitudes can be attributed to possible differences in implementation of dispersive materials in both solvers, as currently investigated.

A second reflected pulse can be observed in the late-time part of the response. This pulse is the reflection off the open boundary conditions at the basis of the phantom. The differences between FVTD and FIT are attributed to different arrangements of the perfectly-matched absorbers used to truncate the computational domain.

C. Comparison with measured results.

A comparison between simulated and measured tumour responses is presented in Fig. 6. Detailed description of the measurement setup can be found in [1,2]. Similarly as in simulations, the measurement was performed on an homogeneous breast phantom with 2 mm thick skin layer.

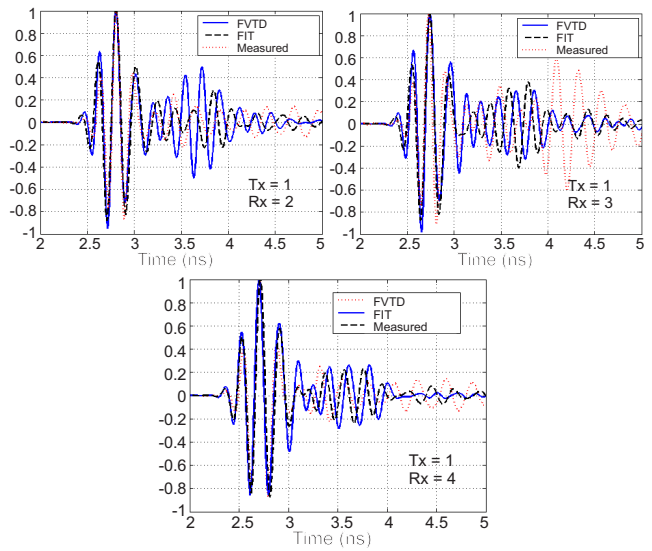

Fig. 6. Time-aligned and normalized tumour's response for different antennas pairs.

The permittivity of all materials from the physical phantom was measured and used as a basis in deriving Debye models used in simulations.

All selected pulses were time aligned and normalized. The results show an excellent agreement between simulated and measured results in regard to the first-arriving tumour reflection pulse. Late-time discrepancies are due to different domain terminations in simulations and obviously in measurements, e.g. because of the plastic shell covered with absorbing material.

V. Conclusion

In this work we presented modelling and results from the large-scale EM simulations of a 31-element antennas array for breast cancer imaging. Two distinct computational methods, FIT and FVTD, were used. The array was used to illuminate and record the backscattered response from a 6 mm spherical tumour phantom embedded in a homogeneous breast model. Dispersion of breast tissues was fully accounted for in the simulations. We obtained comparable results for both solvers. Moreover, a good agreement between simulations and measured results was achieved. Our results are encouraging and important for further advances in microwave imaging techniques. The agreement between simulated and measured results is especially welcomed when considering the challenges associated with the simulation, and in view of future development in microwave tomography, which will require precise modelling of the physical imaging hardware.

Acknowledgement

M. Klemm acknowledges the support of the UK's Engineering and Physical Sciences Research Council (EPSRC). C. Fumeaux acknowledges the support of the Australian Research Council (ARC) under the Future Fellowship funding scheme (FT100100585).

References

[1] M. Klemm, J.A. Leendertz, D. Gibbins, I.J. Craddock, A. Preece, R. Benjamin, "Microwave Radar-Based Breast Cancer Detection: Imaging in Inhomogeneous Breast Phantoms," *IEEE Antennas Wireless Propagat. Lett.*, vol.8, pp.1349-1352, 2009.

[2] M. Klemm, I. J. Craddock, A. Preece, J. Leendertz, and R. Benjamin, "Microwave Radar-based Differential Breast Cancer Imaging: Imaging in Homogeneous Breast Phantoms and Low Contrast Scenarios", *IEEE Trans. Antennas Propagat.*, vol. 58, no.7, pp. 2337-2344, June 2010.

[3] M. Klemm, *et al*, "Towards contrast enhanced breast imaging using ultra-wideband microwave radar system," *IEEE Radio and Wireless Symposium (RWS)*, pp. 516-519, Jan. 2010.

[4] J.D. Shea, S.C. Hagness, B.D. Van Veen, "Hardware acceleration of FDTD computations for 3-D microwave breast tomography," *IEEE Antennas Propagat. Soc. Int. Symp. 2009, APS-URSI '09*, pp. 1-4, 1-5 June 2009.

[5] D. Gibbins, M. Klemm, I.J. Craddock, J.A. Leendertz, A. Preece, R. Benjamin, "A Comparison of a Wide-Slot and a Stacked Patch Antenna for the Purpose of Breast Cancer Detection," *IEEE Trans. Antennas Propagat.*, vol.58, no.3, pp. 665-674, March 2010.

[6] M. Klemm, C. Fumeaux, Dirk Baumann, I.J. Craddock, "Time-Domain Simulations of a 31-Antenna Array for Breast Cancer Imaging", *to be presented at the IEEE Antennas Propagat. Soc. Int. Symp. 2011, APSURSI '11*, 4-7 July 2011.

[7] T. Weiland, "A Discretization Method for the Solution of Maxwell's Equations for Six-Component Fields", *Electronics and Comm. AEUE*, vol. 31, no. 3, pp. 116–120, 1977.

[8] A. Taflove and S. C. Hagness, Computational Electrodynamics: The Finite- Difference Time-Domain Method, 3rd ed. Norwood, MA: Artech House, 2005.

[9] P. Bonnet, X. Ferrieres, B. Michielsen, P. Klotz, and J. Roumiguieres, Chap. 9., Time Domain Electromagnetics, Academic Press, 1999.

[10] J. S. Hesthaven and T. Warburton, Nodal Discontinuous Galerkin Methods: Analysis, Algorithms, and Applications. Springer-Verlag, Berlin, Germany, 2008.

[11] C. Fumeaux, D. Baumann, and R. Vahldieck, "Finite-Volume Time-Domain analysis of a cavity-backed Archimedean spiral antenna", *IEEE Trans. Antennas and Propagat.*, vol. 54, no. 3, pp. 844-851, March 2006.

[12] D.K. Firsov and J. LoVetri, "FVTD - Integral Equation Hybrid for Maxwell's Equations", *Int. J. Numer. Model.*, vol. 21, pp. 29-42, 2007.

[13] A. Chatterjee and R. S. Myong, "Efficient implementation of higher-order finite volume time-domain method for electrically large scatterers," *Progress In Electromagnetics Research B*, vol. 17, 233-254, 2009.

[14] C. Fumeaux, D. Baumann, P. Leuchtmann, and R. Vahldieck, "A generalized local time-step scheme for efficient FVTD simulations in strongly inhomogeneous meshes", *IEEE Trans. Microwave Theory Tech.*, vol. 52, no. 3, pp. 1067-1076, March 2004.

[15] D. Baumann, C. Fumeaux, C. Hafner, and E.P. Li, "A modular implementation of dispersive materials for time-domain simulations with application to gold nanospheres at optical frequencies", *Optics Express*, vol. 17, no. 17, pp. 15186-15200, August 2009.

[16] C. Fumeaux, K. Sankaran, and R. Vahldieck, "Spherical perfectly matched absorber for finite-volume 3-D domain truncation", *IEEE Trans. Microwave Theory Tech.*, vol. 55, no. 12, pp. 2773-2781, December 2007.